Automotive and Engine Technology (2022) 7:353–368
https://doi.org/10.1007/s41104-022-00119-3

ORIGINAL PAPER

Modelling of the NO_x storage behaviour during cold start of modern zeolite SCR catalysts

Deinhofer Lukas[1] · Maurer Michael[1] · Barnstedt Gert[1] · Keber Andreas[1]

Received: 25 April 2022 / Accepted: 7 September 2022 / Published online: 23 September 2022

Abstract

Further stringent emission regulations of modern diesel engines call for a more precise prediction of NO_x emissions, thus enabling a better control of the exhaust-gas aftertreatment systems. A major part of the NO_x emissions is emitted before the light-off temperature of the selective catalytic reduction (SCR) catalyst is reached. Therefore a precise emissions prediction is necessary during the cold start phase of a diesel passenger car. Recent measurements show that NO_x emissions can be stored in the SCR catalysts during cold start. Furthermore a part of this stored NO_x can be reduced during the driving cycle. This paper describes an empiric model predicting the NO_x storage behaviour during vehicle cold start. In a previous work the main influence parameters on the NO_x storage behaviour were investigated on a synthetic gas test bench. The knowledge gained from the previous research work defines the necessary input parameters for the NO_x storage model. These investigations showed that the NO_x storage effect strongly depends on the ammonia (NH_3-) level stored in the catalyst, exhaust-gas mass flow, the water adsorbed (H_2O) on the catalyst, and the temperature of the catalyst. The model was implemented for on-filter and flow-through SCR catalysts. There are two similar models, one for the close-coupled SCR system and the other one for the underfloor SCR system. Each NO_x storage model is split into an adsorption part and a desorption part. For both parts the pre-conditioning from the previous driving cycle is taken into account, which means that the catalyst state at the end of the last driving cycle initializes the model data for the current cycle, in consideration of the downtime between the two cycles. The desorption part calculates the NO_x conversion amount and defines the desorption mass flow of NO_x resulting from the NO_x storage effect. The developed NO_x storage model has been validated with roller dynamometer measurements and with real world driving cycles.

Keywords Cold start NO_x emissions · Real driving emissions · NO_x storage behaviour · NO_x reduction · NO_x adsorption · NO_x desorption · SCR catalyst

Abbreviations

ASC	Ammonia slip catalyst
CO	Carbon monoxide
CO_2	Carbon dioxide
DOC	Diesel oxidation catalyst
DPF	Diesel particulate filter
ECU	Engine control unit
HC	Hydrocarbons
HNCO	Isocyanic acid
H_2O	Water
$(NH_2)_2CO$	Urea
N_2	Nitrogen
NH_3	Ammonia
NO	Nitrogen oxide
NO_2	Nitrogen dioxide
NO_x	Nitrogen oxides
PEMS	Portable emission measurement systems
PM	Particulate matter
O_2	Oxygen
SCR	Selective catalytic reduction

1 Introduction

To meet future stringent emission limits with focus on real driving emissions legislations (RDE), a further technological improvement of the exhaust aftertreatment hard- and software is needed. A typical hardware setup of an aftertreatment system for modern diesel vehicles has a variety

✉ Deinhofer Lukas
Lukas.DA.Deinhofer@BMW.com

[1] BMW Motoren GmbH, Entwicklung Dieselmotor, Steyr, Austria

of different catalytic converters installed. A state of the art diesel passenger vehicle exhaust aftertreatment system consists of a diesel oxidation catalyst (DOC), a diesel particulate filter (DPF) with SCR coating, a selective catalytic reduction catalyst (SCR), and an optional NH3 slip catalyst (ASC). [1–3]

However this complex setup of different hardware components leads to a challenge in modelling those exhaust aftertreatment components. Furthermore the different components influence each part of the exhaust aftertreatment system downstream with respect to the modelling and performance behaviour. In order to implement an emission model of each system component in the engine control unit (ECU) an overall understanding and the interaction of each system is necessary. For example to reduce the HC and CO emissions a DOC is installed upstream in the exhaust system. As it reaches its light-off temperature, the DOC helps to heat up the components downstream due to its exothermic oxidation reaction. [4].

For optimum control of the SCR system a lot of different model types are needed to depict the ongoing process in an SCR catalyst, such as the NH_3 storage behaviour [5, 6], ageing effects [7], oxidation processes [8] and so on. [9, 10]

In order to enable fast heating up of the SCR catalyst, so it reaches its light off point earlier, a diesel particulate filter (DPF) in close-coupled position with an SCR coating is used [11]. The combination of these features allows a better packaging because less overall volume is needed [12]. The improved heating up of the SCR on-filter layout, leads to an improved cold start emission behaviour [10, 13].

Combining an on-filter SCR catalyst with a second flow-through SCR catalyst in the underfloor offers a better NO_x reduction potential at higher operating temperatures, occurring at high load driving cycles and during DPF regeneration. Combining two SCR catalytic systems in one exhaust aftertreatment system also increases the overall functional SCR volume. The system efficiency can be further increased by mounting two separate urea dosing valves for each catalyst, offering an optimized usage of the dosed urea and providing the optimal urea amount in each catalyst depending on the driving situation. Two urea dosing units in combination with an intelligent control unit enable a lower NH_3 oxidation in high dynamic driving conditions such as the DPF regeneration. [14]

Currently, the most effective way to reduce NOx emissions from lean-burn diesel engines is using a SCR catalyst [15, 16]. Beyond the light-off temperature the general SCR procedure is well known and there are several models describing the catalytic behaviour in this temperature region [16–18]. Furthermore the different reaction mechanisms needed for the SCR reactions to take place have been studied thoroughly by a variety of research groups [19, 20].

Due to the lean combustion of the diesel engine, a reducing agent is needed in the catalytic process of the SCR system [21]. In stationary applications often pure ammonia is used [22]. However, for mobile applications pure ammonia is not suitable due to safety and storing reasons, because of its toxic, corrosive and flammable characteristics [23]. An aqueous solution of water and urea, so called AdBlue®, enables the SCR catalysis for the mobile application. There are three main steps needed to release the ammonia from the urea solution in a gaseous state for the SCR reaction. In the first reaction step the water in the aqueous solution evaporates (1), after this the thermolysis (2) of the urea generates ammonia and isocyanic acid. In the last step the hydrolysis (3) of the isocyanic acid with water urea reacts to ammonia and carbon dioxide. [23–25]

$$\text{evaporation}: (NH_2)_2CO_{(aq)} \rightarrow (NH_2)_2CO_{(l)} + 6.9H_2O_{(g)} \tag{1}$$

$$\text{thermolysis}: (NH_2)_2CO_{(l)} \rightarrow NH_{3(g)} + HNCO_{(g)} \tag{2}$$

$$\text{hydrolysis}: HNCO_{(g)} + H_2O_{(g)} \rightarrow NH_{3(g)} + CO_{2(g)} \tag{3}$$

Furthermore, current small-pore zeolites have multiple storage sites for NH_3 adsorption and desorption. Typically the storage capacity is available at temperatures below 200 °C and decreases with rising temperature. This leads to possible NO_x reactions during cold start because of available NH_3. [26–32]

Depending on the exhaust gas composition in the SCR catalyst, different NO_x reduction reactions take place. There are three main reaction paths, the so-called standard SCR (4), fast SCR (5) and the NO_2 SCR (6) reaction. For the standard SCR reaction only ammonia, nitrogen oxide and oxygen are needed. However, the fast SCR reaction needs an equimolar amount of NO and NO_2. The NO_2 SCR reaction has the big disadvantage, that it has a higher NH_3 consumption compared to the other mentioned reactions. Compared to the fast SCR reaction the standard one starts at lower catalyst temperatures. [30–35].

$$\text{standardSCR}: 4NO + 4NH_3 + O_2 \rightarrow 4N_2 + 6H_2O \tag{4}$$

$$\text{fastSCR}: NO + NO_2 + 2NH_3 \rightarrow 2N_2 + 3H_2O \tag{5}$$

$$\text{NO2SCR}: 6NO_2 + 8NH_3 \rightarrow 7N_2 + 12H_2O \tag{6}$$

The transport sector is one of the leading sectors in CO_2, NO_x and PM emissions [33]. Currently the diesel engine plays a major role in the transport sector, highlighting the need for lower emissions of those vehicles [34]. The world harmonized light vehicle test procedure (WLTP) and the real driving emissions regulation (RDE) lead to a more complex legislation in Europe [35]. Additionally other countries such as China, Brazil and India, are also introducing more stringent emissions regulations in the next couple of years [36]. Furthermore there will be a greater focus on the cold start in RDE cycles, with extended temperature regions [37]. A large portion of the NO_x emissions occur during the vehicle cold start. During cold start conditions the SCR exhaust aftertreatment system has major drawbacks[38, 39]. The low catalyst temperatures lead to a strongly reduced NO_x conversion rate [38, 39]. On the one hand a fast heat-up of the catalysts keeps the NO_x emissions to a minimum, on the other hand it comes at the expanse of CO_2 emissions.

Under dry conditions modern SCR catalysts show the possibility of storing NO_x during cold start and partially reducing those during heat-up [40, 41]. This NO_x reduction potential is depending on pre-conditioning of the SCR catalyst, therefore it cannot directly be controlled [42]. However, there are several research works directed at optimizing the NO_x storage effect by adapting the chemical composition of the washcoat [43–45]. To meet future emission regulations bigger overall catalyst volumes are needed. The absolute amount of NO_x storage capacity scales with the volume of the catalyst.

The basic influence parameters on the NO_x storage effect have been studied in a previous study [42]. This work focuses on the modelling of the NO_x storage effect for implementation in the ECU. The effects of the NO_x storage behaviour have first been seen during vehicle measurements and have successfully been replicated on a synthetic gas test bench for a Cu-zeolite. As long as the SCR catalyst is dry and cold, NO_x can be adsorbed, leading to zero tailpipe NO_x emissions. However, as water steam from the exhaust gas upstream of the exhaust system reaches the SCR catalyst, it condensates on the zeolite and causes a sudden temperature rise. The water in the exhaust gas originates from the burned fuel and the water content of the intake air. This temperature increase subsequently causes the NO_x adsorption to end, followed by a partial desorption of the stored NO_x emissions. The rest of the stored NO_x is reduced by the available NH_3 on the catalyst. This entire process lasts from a few seconds up to a couple of minutes, depending on the exhaust-gas mass flow, water concentration in the exhaust gas and temperature. Furthermore condensed water on the catalyst strongly inhibits the NO_x storage capacity and drastically reduces the time need for the whole process. [42]

The modelling of the NO_x storage behaviour enables a better utilization of the CO_2-NO_x trade-off, by increasing the robustness of the modelled NO_x during cold start. Furthermore, this model aims to improve the signal quality for the ammonia dosing strategy, by correcting the NH_3 storage level by the amount of the converted part of the stored NO_x during cold start. Therefore, the model corrects the NH_3 storage in a way that both possible dosing errors generated by the NO_x storage behaviour can be avoided. An overdosing can cause NH_3 slip and an underdosing may lead to a reduced NO_x reduction.

Beyond this the worst-case scenario is that the SCR catalyst has a high amount of preloaded NO_x at the beginning of the vehicle cold start. In this scenario the cumulated NO_x emissions after the catalyst can exceed the upstream NO_x emissions during the desorption phase. Such a high NO_x preloading can be caused by a preconditioning with only long idle times or short vehicle manoeuvres. An exemplary measurement with a worst-case preconditioning can be seen in Fig. 1. The preconditioning causes the absence of the adsorption phase of the NO_x storage effect for the close-coupled SCR system. However for both SCR systems a preabsorbed amount of NO_x is emitted during the desorption phase. At the first cursor position the end of the desorption phase of the close-coupled SCR system is reached and the cumulated NOx emissions of the up- and downstream of the SCR system are almost the same. The underfloor SCR system exceeds the cumulated engine out NO_x emissions during the desorption phase. This leads to very high overall NO_x emissions during the cold start phase. At the second cursor position the end of the desorption phase of the underfloor SCR system is reached. The higher NO_x emissions caused by a worse preconditioning lead to an overall negative impact to meet future stringent emission regulations.

2 Modeling

2.1 Requirements

As mentioned above the model shall be implemented in the ECU. For the ECU model an empirical model approach has been chosen, due to its short computation time and lower power requirements. The use of constants, 2D and 3D maps enable the modelling of non-linear behaviour depending on the driving condition. Furthermore, a map-based model offers a more comprehensible calibration process during development.

The aim of this model is to increase the model accuracy for other ECU models by depicting the NO_x storage behaviour during cold start. The main challenge hereby is to fulfil the wide range of RDE boundary conditions.

In order to guarantee the required model quality, the NO_x storage behaviour is implemented for close-coupled SCR systems and the underfloor SCR systems separately. The structural overview of the vehicle exhaust aftertreatment system can be seen in Fig. 2.

Furthermore, gas sampling ports and temperature sensors have been installed in the exhaust aftertreatment components to validate the iterative model calibration process.

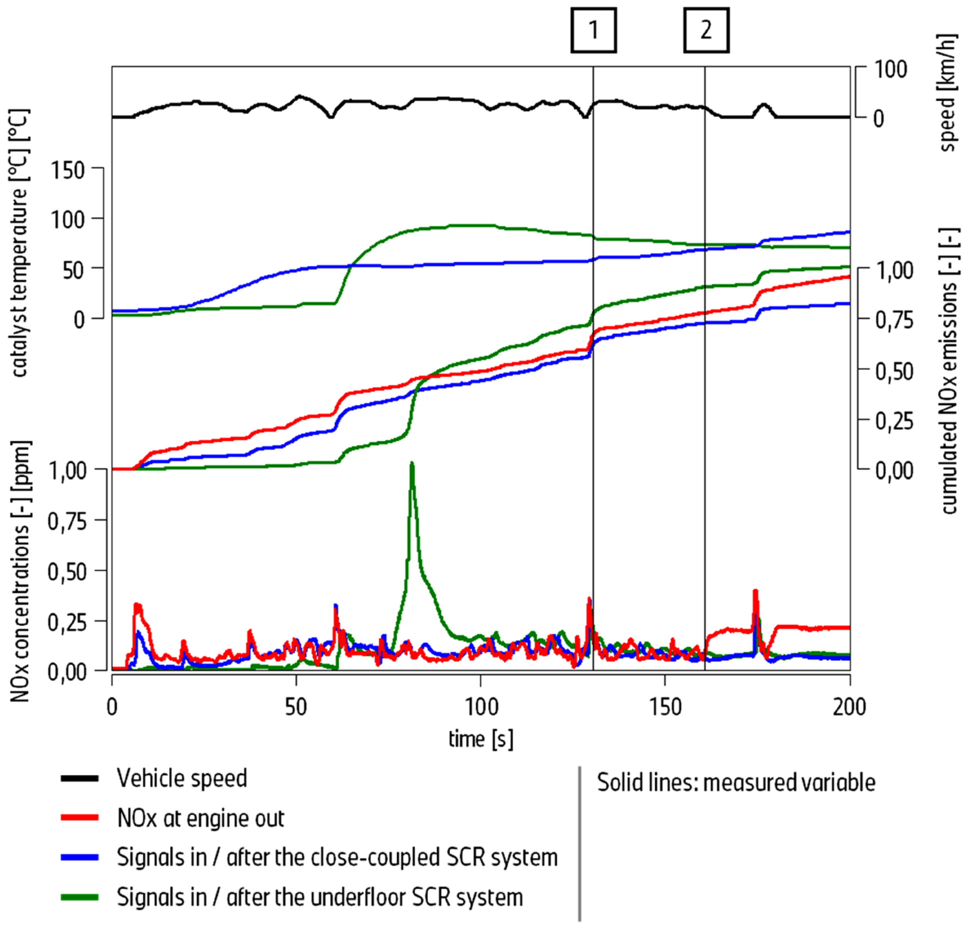

Fig. 1 Test cycle with an exemplary worst preconditioning cycle

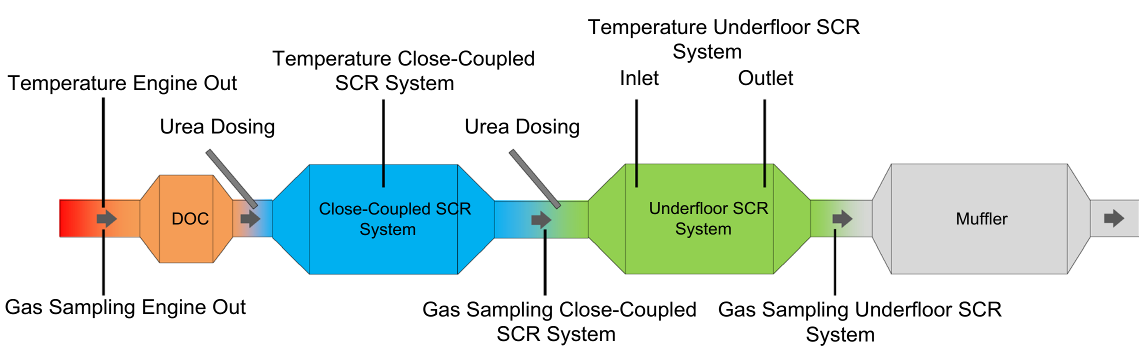

Fig. 2 *Vehicle exhaust aftertreatment components according to Deinhofer* et al. [42]

2.2 Structure

The NO_x storage models for the close-coupled SCR and the underfloor SCR have the same basic structure, despite the parameter sets between the two are clearly different. Basically, the model itself is split into two consecutive parts, the adsorption part and the desorption part. An overview of the basic sequence of the model blocks can be seen in Fig. 3. The main input parameters have been defined by the previous research work [42]. The NO_x storage model uses the NO_x concentration (c_NO_x), the NO_x mass flow (mf_NO_x), the adsorbed water on the catalyst (m_H_2O), the catalyst temperature (T_SCR), the exhaust mass flow (mf_exhaust) and the NH_3 storage level of the catalyst (m_NH_3) as input signals. The model output NO_x concentration as well as the mass flow and the NH_3 storage level are calculated as a result of the NO_x storage behaviour. The calculation of each block is based on characteristic curves and

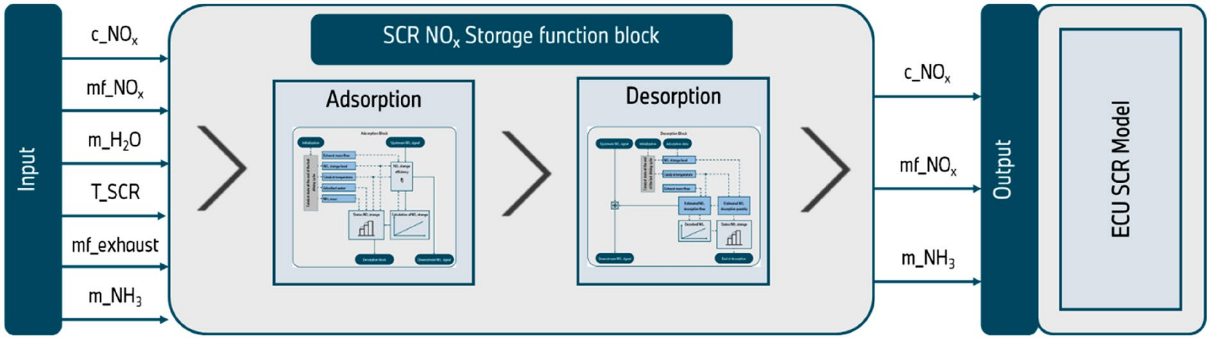

Fig. 3 Basic model sequence of the NO_x storage function

maps, which were supplied by a wide range of previous performed measurements on the roller test bench and during on road tests. In a previous work [42] hydrocarbons and carbon monoxide have been determined as influence parameters. These are not considered in this model, because of missing measurement sensors and adequate modelled values. This could be an addition to the current model for future works.

The adsorption block is positioned before the desorption block. The adsorption block takes the preconditioning caused by the previous driving cycle into account, for example initialize stored NO_x during subsequent short driving cycles. The storage behaviour of the catalyst is regulated by the adsorption block, including possible NO_x slip caused by particular operating conditions. After the adsorption phase, the desorption block of the NO_x storage model is activated. Depending on the operating conditions of the catalyst the amount of desorbed NO_x is calculated. The desorbed NO_x amount is then added to the upstream NO_x signal of the catalyst. The output signals of the SCR NO_x storage function block act as an input signal for the other SCR model blocks in the ECU.

A more detailed view of the adsorption part of the NO_x storage function can be seen in Fig. 4. However, the represented figure still shows a simplified version of the real model, due to the high complexity and the degree of cross-linking of the actual model. At the start of each driving cycle, the catalyst NO_x and NH_3 storage state and the adsorbed water on the catalyst at the end of the last driving cycle is initialised. Additionally, the modelled catalyst temperature is set in compliance with the calculated cool down rate. The adsorption phase is only active if the boundary conditions are true for the initialization block, otherwise the system switches directly to the desorption block.

The adsorption block consists of three subfunction blocks. The NO_x storage efficiency calculates the amount of NO_x slip during the adsorption phase.

The calculated NO_x storage efficiency (μ_{NO_xStor}) is calibrated depending on the exhaust-gas mass flow, the stored amount of NO_x and the catalyst temperature, the storage efficiency is estimated in each driving situation. A high temperature and a greater exhaust mass flow enhances the tendency towards NO_x slip. The NO_x not stored on the catalyst is forwarded to the downstream NO_x signal. A higher temperature reduces the threshold value for the exhaust mass flow towards occurring NO_x slip. Both parameters are input signals for a characteristic map to determine the NO_x storage efficiency. Additionally, the stored NO_x and the catalyst temperature are processed in a characteristic map to calculate the NO_x saturation level of the catalyst in a next step, with a higher saturation level causing the NO_x storage efficiency to decrease. The saturation level is defined as the ratio between the maximal storable amount of NO_x on the catalyst and the current amount of adsorbed NO_x. The maximal storable amount of NO_x on the catalyst is determined in a characteristic map with the temperature and the state of health of the catalyst actin as input parameters. The resulting NO_x storage efficiency factor is then multiplied with the upstream NO_x mass flow ($NO_{x_{Upstream}}$) of the catalyst. The formulas (7) show the calculation of the NO_x mass flow downstream of the catalyst in the adsorption block.

$$NO_x flowtowardsthecatalyst = \mu_{NO_xStor} \bullet NO_{x_{Upstream}} \tag{7}$$

$$DownstreamNO_x signal = (1 - \mu_{NO_xStor}) \bullet NO_{x_{Upstream}} \tag{8}$$

The second subsystem block calculates the NO_x stored by integrating the NO_x signal which is corrected by the NO_x storage efficiency. The currently stored NO_x is returned to the NO_x storage efficiency block and the NO_x storage status block. The status of the NO_x storage capacity represents the third subsystem block, therein a survey at the vehicle start occurs and a continuous query is executed to determine if the adsorption phase is still active. There are two evaluation paths, on the one hand there is a temperature limit and on the other hand there is a maximum NO_x storage capacity. Depending on the driving cycle either one of those paths specifies the end of the adsorption phase. The NO_x storage behaviour is strongly depending on the catalyst temperature.

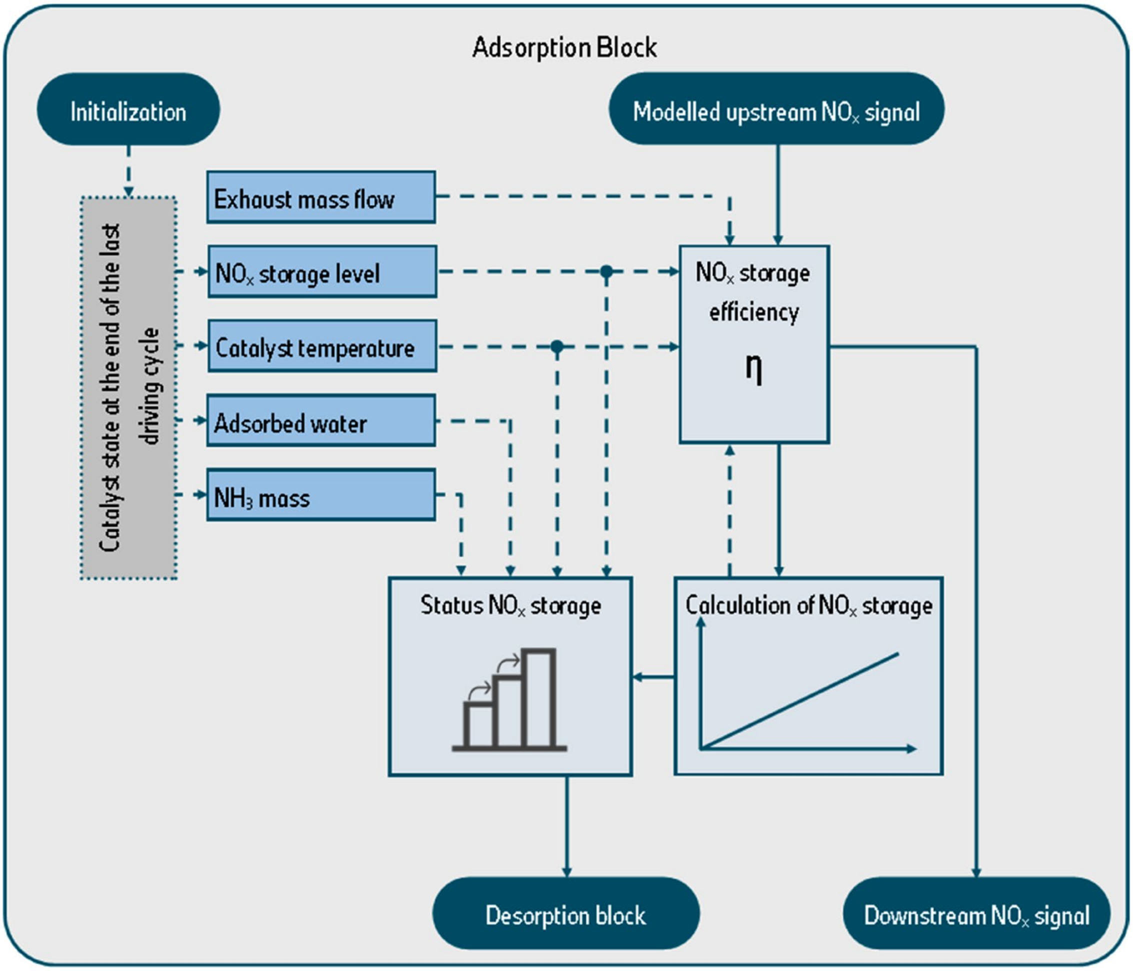

Fig. 4 Simplified overview of the adsorption block

Since an increase in temperature caused by the water adsorption leads to the desorption of the stored NO_x, a catalyst temperature limit is calculated to define the end of the adsorption phase. The amount of adsorbed water on the catalyst influences the limit temperature. With a higher amount of adsorbed water on the catalyst the exothermic behaviour during the water adsorption is reduced. The other limit value is the maximum amount of storable NO_x on the catalyst. The storage capacity depends on the temperature, stored NH_3 on the catalyst, ageing condition and the amount of adsorbed water on the catalyst. With increasing temperature, NH_3 filling level, and amount of adsorbed water, the storage capacity is reduced. Furthermore, with the progressing ageing of the catalyst the storage capacity also decreases. The influence parameters allow the adsorption block to predict the occurring NO_x slip and the duration of NO_x adsorption cycle for varying driving cycles.

The general procedure of the desorption block with the sub-function blocks can be seen in Fig. 5. The desorption block is located downstream of the adsorption block and is activated as soon as the adsorption block status NO_x storage switches over. As in the adsorption block, the values at the end of the last driving cycle are used to initialise the NO_x storage level and catalyst temperature in this block. The catalyst temperature takes the cool down rate between the driving cycles into account. A relevant case for the initialisation phase is when the previous driving cycle ends during the desorption phase. The desorption block uses the NO_x storage level calculated in the adsorption block, the catalyst temperature and the exhaust-gas mass flow as input parameters to define the desorption behaviour of the NO_x storage effect. After the adsorption phase ends, the NO_x storage level together with the catalyst temperature are used to estimate the amount of stored NO_x that can be converted. For the calculation of the converted amount of NO_x the temperature of the catalyst for different positions along the flow direction is determined. A higher average catalyst temperature leads to a higher conversion rate of the stored amount of NO_x. Furthermore the presence of stored NH_3 enables the NO_x conversion during the desorption phase. A higher amount of stored

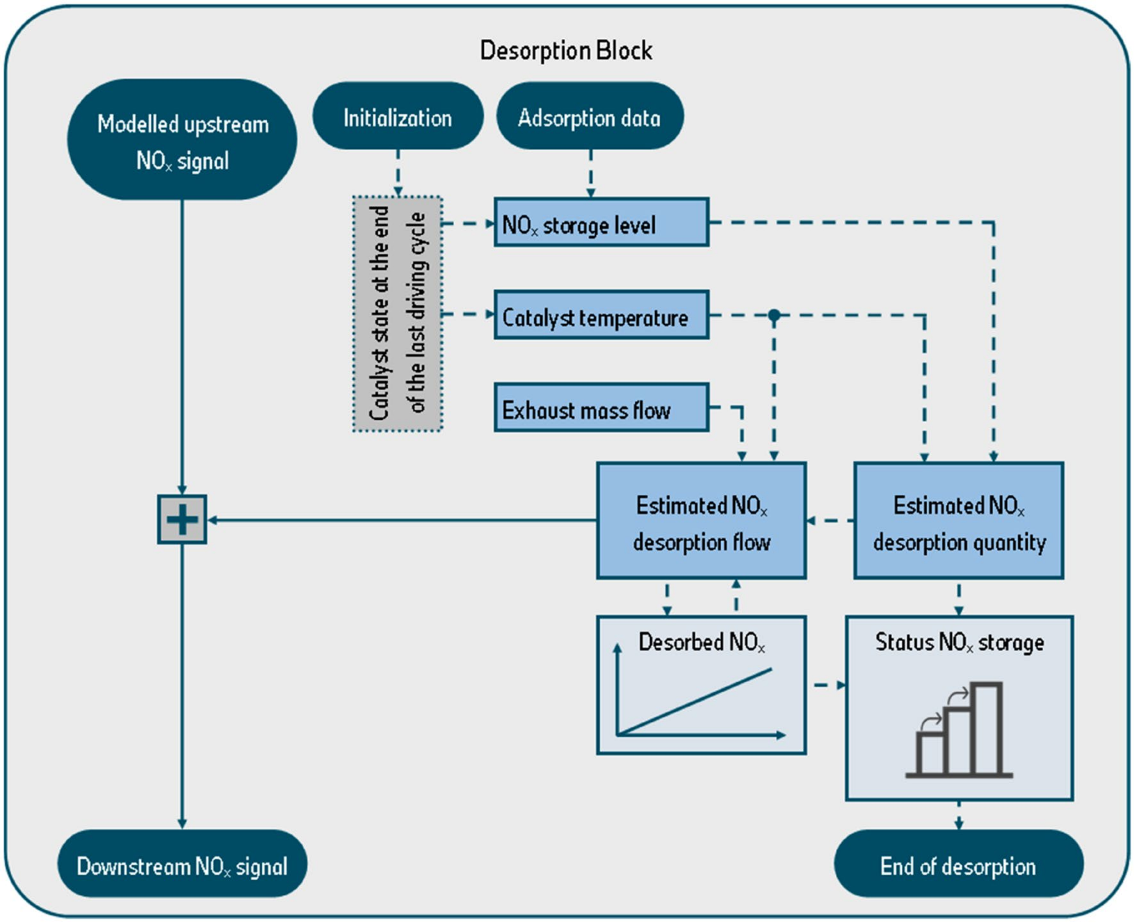

Fig. 5 Simplified overview of the desorption block

NO_x emissions leads to a higher NO_x conversion rate, this is based on a series of vehicle measurements. The quantity of stored NO_x at the end of the adsorption phase correlates with the dynamic driving behaviour and the water input on the catalyst during the cold start phase. Therefore the NO_x storage level and the average catalyst temperature are used to define the NO_x conversion rate in a characteristic map. The NO_x conversion rate is then multiplied with the NO_x storage level to calculate the amount of converted NO_x for the desorption phase. The calculation process for determining the amount of converted NO_x and desorbed NO_x amount are similar to the formulas (7). The calculated NO_x desorption mass flow depends on the NO_x storage level in the catalyst, the catalyst temperature and the relative NO_x desorption amount. The exhaust mass flow adapts the NO_x desorption mass flow in case of a standstill time of the engine or during very high exhaust mass flows.

The catalyst temperature and the relative NO_x desorption amount define in a characteristic map for each timestep the current NO_x desorption mass flow. The calculated NO_x desorption mass flow reduces the increases NO_x desorption amount, which acts as a recursively input parameter for the NO_x desorption mass flow calculation. The modelled NO_x desorption flow allows to depict the real desorption process by adding the estimated NO_x desorption flow to the upstream NO_x signal. Leading to an increase of the NO_x emissions after the catalyst during the desorption phase. The relative NO_x desorption amount is formed by the ratio between the estimated desorption quantity and the cumulated estimated NO_x desorption flow. Furthermore, the calculated ratio defines the status of the desorption phase, as the accumulated desorbed NO_x amount reaches the estimated maximum NO_x desorption quantity, the desorption phase ends.

The previously mentioned influence parameters of the model can assess the actual behaviour of the NO_x emissions during vehicle cold starts, caused by the NO_x storage effect. This leads to an improved signal quality for other SCR models in the ECU in a broad RDE area. To meet future stringent emission regulations vehicles may have to degrade the engine power during the cold start, therefore a better modelling of the cold start emissions allows an improved behaviour for the customer.

2.3 Model Validation

For the model validation process a variety of vehicle measurements were carried out, from which only the most significant ones can be discussed here. Among others, a variation of the vehicle conditions and the environmental conditions were conducted. Different preconditioning driving cycles were used, with different environmental temperatures, driving distance, average vehicle speed and dynamic behaviour. During the actual test cycle the parameters mentioned before were also varied. One result of this test variation was that the amount of adsorbed water on the catalyst was identified to have a significant influence on the NO_x storage behaviour. This behaviour is in accordance with previous research work on the synthetic gas test bench. For the validation of the SCR NO_x storage function, roller test bench and RDE measurements have been carried out.

2.4 Roller Test Bench Measurement

To evaluate the performance of the NO_x storage model two different preconditioning cycles and two diverse driving cycles were used. The characteristic values of each cycle is displayed in the Table 1 and the corresponding test matrix can be seen in Table 2. The dynamic factor is the averaged modulus of the product between the acceleration and vehicle speed. For the preconditioning cycles the dynamic factor has been determined for the entire test cycle, whereas the dynamic factor of the test cycle has been calculated for the first 300 s. The formula (9) was used to calculate the dynamic factor with the vehicle velocity and the acceleration as input parameters. The defined city cycles were derived from real-world driven routes, those depict the upper and lower dynamic spectrum of typical driving scenarios during rush hour and a city ride. Due to the major influence of the adsorbed water on the catalyst, two different preconditioning cycles were chosen. The difference of these two preconditioning cycles is the catalyst temperature for each SCR system, leading to a varying amount of adsorbed water on the catalyst. The low dynamic cycle aims for low catalyst temperatures to adsorb as much water as possible on the catalyst. For the high dynamic cycle a high temperature in the exhaust aftertreatment system has been achieved to guarantee a very low amount of water adsorbed on the catalysts.

$$Dynamicfactor = \frac{1}{t}\sum_{i=1}^{t}\left|v_{(t)} \bullet a_{(t)}\right| \tag{10}$$

Furthermore, the dynamic driving behaviour has an influence on a variety of factors in the NO_x storage behaviour. The affected parts are the NO_x storage efficiency, NO_x storage amount and NO_x desorption amount. Therefore, two driving cycle variants were tested, with regard to the dynamic performance.

The high dynamic preconditioning cycle guarantees a minimum of adsorbed water on the catalyst to evaluate the model performance under dry conditions with high repeatability. The main difference between the preconditioning cycles are the average catalyst temperatures for both catalyst systems. For the preconditioning cycles the difference in average catalyst temperature is 117 K for the close-coupled SCR and 156 K for the underfloor SCR. The low dynamic driving cycle feeds a large quantity of water into the exhaust aftertreatment system at low operating temperatures, causing a high amount of preloaded water on the catalyst. The testing procedure, with the preconditioning cycle, the cool down phase, and the driving cycle can be seen Fig. 6.

Table 1 Characteristic values of each cycle for preconditioning and testing on the roller test bench

	Ø-Vehicle speed	Dynamic factor
Low dynamic cycle	18.1 km/h	5.1
High dynamic cycle	101.0 km/h	17.4
Low dynamic city cycle	10.9 km/h	6.4
High dynamic city cycle	32.6 km/h	16.0

Table 2 Testing matrix for the roller test bench measurements

Test	Preconditioning	Driving cycle
1	High dynamic cycle	Low dynamic city cycle
2	Low dynamic cycle	Low dynamic city cycle
3	High dynamic cycle	High dynamic city cycle
4	Low dynamic cycle	High dynamic city cycle

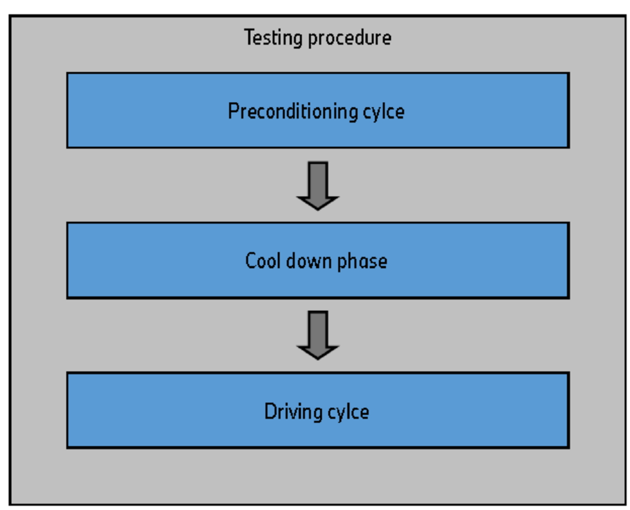

Fig. 6 Testing procedure for roller test bench measurements

The tested vehicle has been equipped with additional temperature sensors and exhaust gas sample ports as can be seen in Fig. 2. During the chassis dynamometer tests further exhaust gas analysers were installed. This allows to check the signal quality of the added sensors in the test vehicle and guarantees a precise model evaluation.

The first test with a high dynamic cycle as a precondition and a low dynamic test cycle can be seen in Fig. 7. The typical behaviour of the NO_x storage effect can be seen with the absence of the NO_x emissions after each catalyst system until the water adsorbs on the catalyst causing the sudden rise in temperature. This behaviour is consistent to what can be found in the literature [2, 40, 42, 45]. To enhance readability the model variables (dotted lines) have only been added to the cumulated NO_x emissions. Due to the ongoing development process the cumulated NO_x emissions and the NO_x concentrations have been normalized. The cursor 1 and cursor 2 mark the end of the desorption phases and the NO_x storage phases for the close-coupled (1) and underfloor SCR system (2). As can be seen for both catalyst systems, no NO_x slip occurs during the adsorption phase, which is valid for the measured and the modelled NO_x signal. The dry condition and the low dynamic properties during the city cycle drastically reduce the tendency towards NO_x slip during the adsorption phase, which coincides with previous research works. Furthermore, both criteria allow a very long adsorption phase for both SCR catalyst systems. In general the timing of the start of the desorption phase of the model matches the reality very well and is consistent with the rise in temperature. However, for the close-coupled SCR system the timing shows a slight tendency towards a too early start of the desorption phase. Additionally, the calculated NO_x reduction is slightly lower, leading to a higher amount of desorbed NO_x emissions. The modelled desorption mass flow matches the measured one, because of the similar slopes in cumulated NO_x emissions of both curves. Up to now during the cold start the model approach did not consider the NO_x storage effect. This caused that the modelled NO_x signals after the close-coupled and underfloor SCR systems were similar to the modelled NO_x engine out signal. Therefore, the newly developed NO_x storage model brings an improvement in picturing the real behaviour during vehicle cold starts. Beyond that in this driving cycle a high NO_x reduction has occurred during the cold start, which can be seen at the position of cursor 2. The overall reduction amount can be seen as the difference between the cumulated

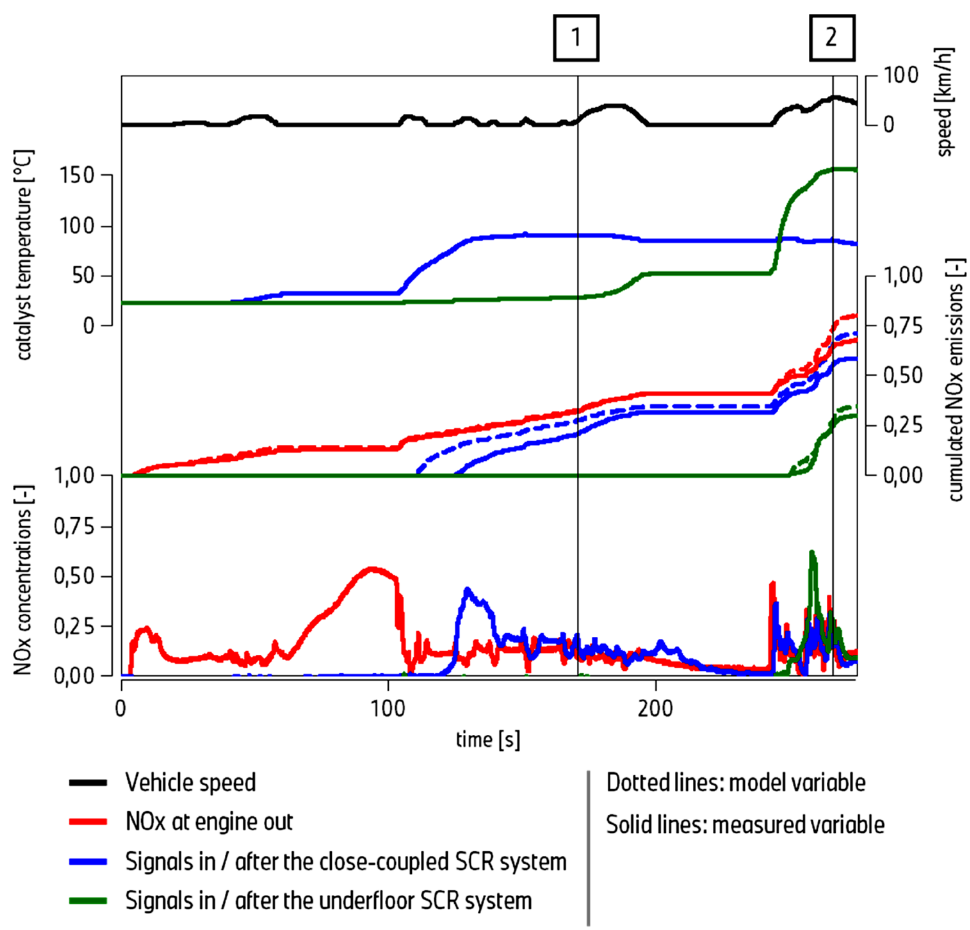

Fig. 7 Test 1 with high dynamic preconditioning and low dynamic city cycle roller test bench measurement (normalized NO_x values)

engine out NO_x emissions and the cumulated NO_x signal after the underfloor SCR system.

For the second test the same low dynamic driving cycle was investigated, however a low dynamic preconditioning cycle was used. This allows the comparison of two different preconditioned states for the same low dynamic city cycle. The higher preloading of water on the catalyst causes a reduced exothermic behaviour leading to a lower rise in temperature during the water adsorption. The lower temperature at the desorption begin results in a lower NO_x reduction potential. This theory can be seen in Fig. 8, for both cursor positions of the catalyst systems. Furthermore, the higher water preloading reduces the maximum amount of storable NO_x, combined with the lower rise in temperature causing an earlier end of the adsorption phase during the cold start. That kind of behaviour can be seen by comparing Test 1 and Test 2, the overall NO_x reduction is drastically reduced due to the higher water preloading. The higher water preloading significantly reduces the rise in temperature during the water adsorption. This is predominantly the case for underfloor SCR systems. A possible reason for this is that the underfloor SCR system has a greater zeolite volume. Moreover, the higher water preloading first effects the upstream components of the exhaust aftertreatment system. For the close-coupled SCR system the start of the desorption phase as well as the desorption NO_x flow of the model does not fit the measurement signal precisely. The calculated amount of NO_x desorption is slightly higher than in reality as can be seen at cursor 1. This cannot be applied to the underfloor model, where the desorption starts slightly delayed in model compared to the measurement and the NO_x desorption flow also does not match the measurement curves. However, at the second cursor the cumulated amounts of NO_x after the underfloor SCR system are nearly the same, which means that the cumulated amount of desorbed NO_x is calculated correctly. These discrepancies of the model compared to the real behaviour can be further reduced by the ongoing development process of parametrising the model. Overall the NO_x storage model increases the NO_x model accuracy during cold start.

The test in the high dynamic city cycle and the high dynamic preconditioning is displayed in Fig. 9. The high dynamic cycle distinguishes from the low dynamic cycle by higher operating vehicle speed and less as well as shorter vehicle stops. The higher dynamics causes NO_x slip during the adsorption phase of the close-coupled SCR system, as

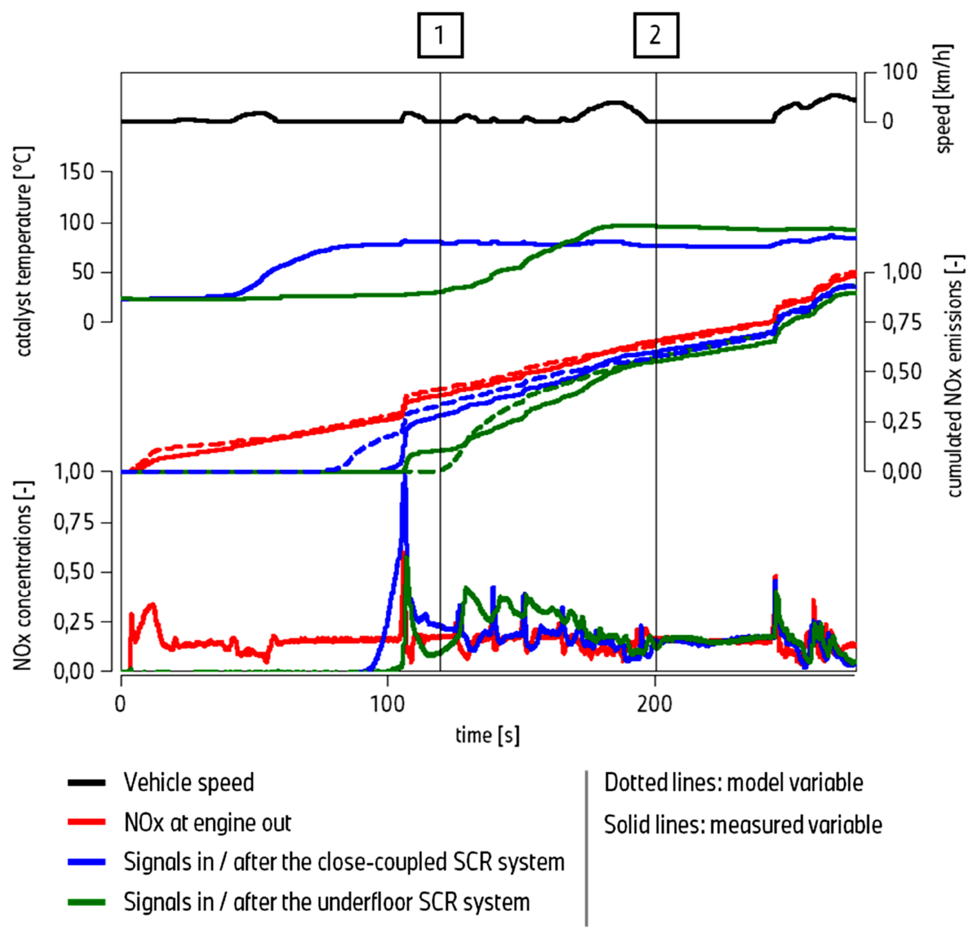

Fig. 8 Test 2 with low dynamic preconditioning and low dynamic city cycle roller test bench measurement (normalized NO_x values)

Fig. 9 Test 3 with high dynamic preconditioning and high dynamic city cycle roller test bench measurement (normalized NO_x values)

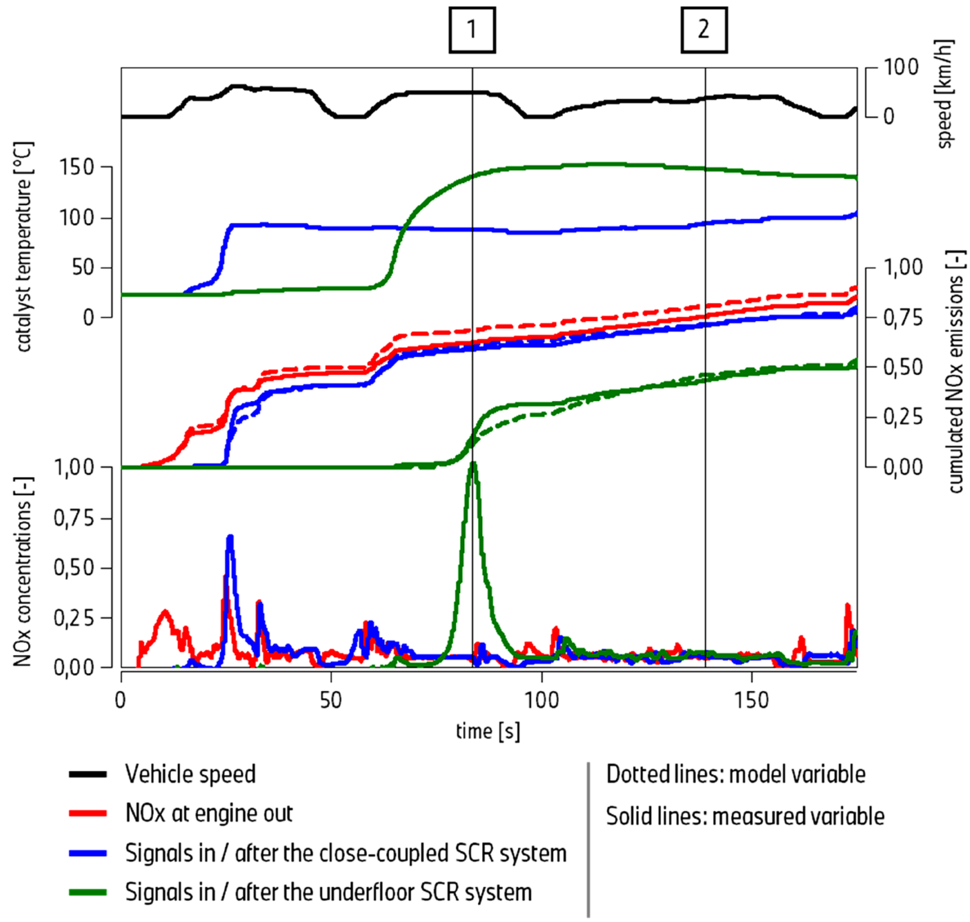

the temperature increases. The occurring NO_x slip during the first acceleration leads to a small peak in the NO_x concentration downstream of the close-coupled SCR system. For the underfloor SCR system, the same behaviour can be observed, the NO_x slip arises during the second acceleration block at about 65 s. Both NO_x slip events can be represented by the NO_x storage model. Also, during the high dynamic city driving cycle a more pronounced desorption peak than in lower dynamic driving cycles occurs. In general, a proportionally lower NO_x reduction caused by the NO_x storage effect can be observed in Test 3. For the higher dynamic driving behaviour, a greater quantity of diesel fuel is needed, which leads to a greater amount of water in the exhaust gas. This causes an earlier and more pronounced rise in temperature. The start of the desorption phase as well as the calculated amount of NO_x desorbed matches the measurements very well. The NO_x desorption mass flow shows a slight difference in the descending flank of the desorption peak, however for both systems the modelled values are lower in comparison to the measured ones. Overall the NO_x storage process matches quite well for these boundary conditions.

For the fourth test cycle, the NO_x storage behaviour is similar to the second test cycle due to the same preconditioning cycle. The low dynamic preconditioning causes a less distinctive NO_x desorption peak for the underfloor SCR system, which can be seen in Fig. 10. The desorption peak of the downstream SCR system is wider and decreased in height. Furthermore, the rise in temperature due to the water adsorption is also more blurred and decreased for both catalyst systems, this behaviour is more pronounced in the underfloor SCR system. A possible reason for this can be differences in the relative water saturation, catalyst volume, and/or amount of washcoat. This reduced exothermic behaviour diminishes the NO_x conversion rate immensely, similar to the second test cycle. Additionally, the occurring NO_x slip during the NO_x adsorption phase is similar to the drier preconditioned test cycle. It stands out that the cumulated modelled engine out NO_x emissions have an offset after the first acceleration. It is noteworthy that the shown modelled values are derived from an early state of an ongoing development process, therefore slight discrepancies can occur for some input signals. Due to the offset of the cumulated modelled NO_x emissions, the cumulated NO_x values for both catalyst systems also exhibit an offset to the measured curves. Despite that, the model accuracy of the NO_x signal during the cold

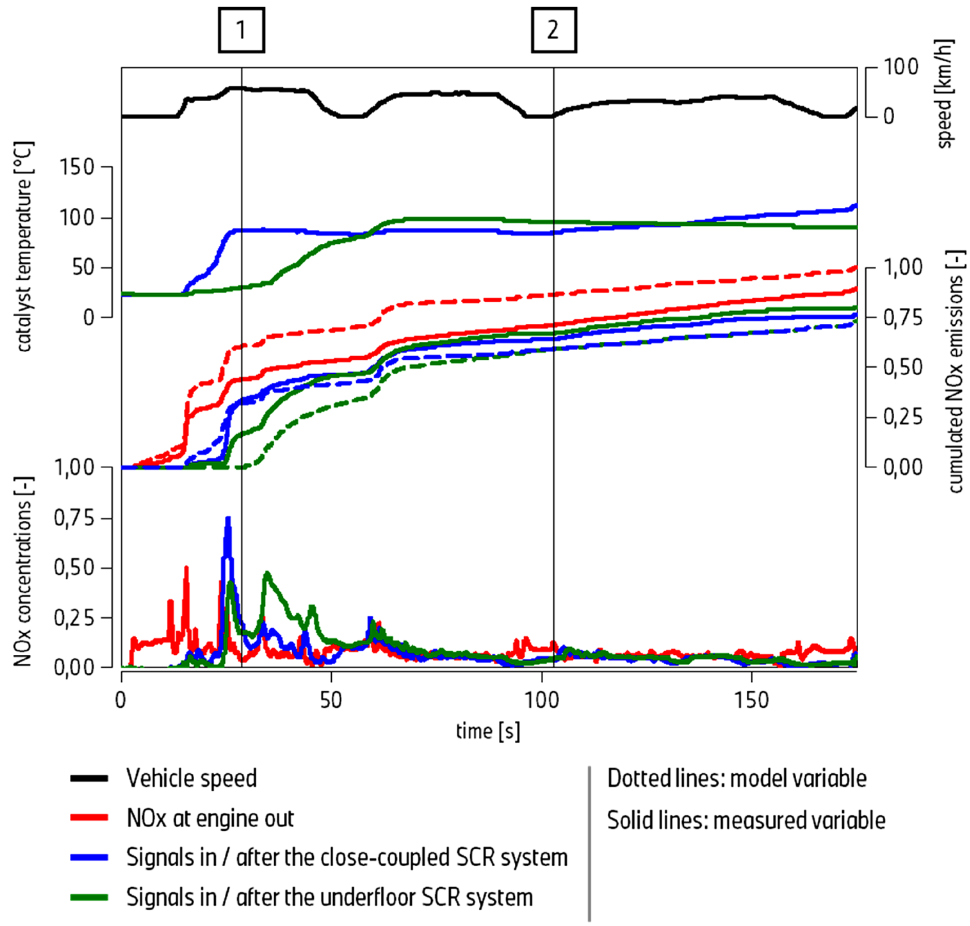

Fig. 10 Test 4 with low dynamic preconditioning and high dynamic city cycle roller test bench measurement (normalized NO_x values)

start still reveals an improvement, compared to the previous system behaviour.

Additionally, further roller test bench measurements in the two preconditioned states were performed. All these measurements showed an improvement of the model accuracy during the cold start. The benchmarking of the NO_x storage model was performed on a variety of model derivates and diesel engine types. Overall, the performed roller test bench measurements highlighted the performance and model accuracy of the NO_x storage model.

2.5 RDE Measurement

For further validation of the NO_x storage model, RDE driving cycles were performed. The result of one RDE measurement can be seen in Fig. 11. The tested vehicle was equipped with a portable emission measurement system (PEMS) similar to the measurement technology of the roller test bench vehicles, thus enabling an evaluation of the model performance quality. The shown section of the RDE driving cycle consists of a short stationary phase (35 s), followed by a brief city phase (60 s) and ends with an extra urban highway phase (105 s). The distinctive temperature curves are similar to the roller test bench measurements with the high dynamic preconditioning cycle. The start of the desorption phase of the close-coupled SCR system is slightly earlier in the model, however the desorption mass flow and the NO_x conversion rate at the first cursor point matches very well with the measurements. At the second cursor point the overall NO_x reduction is consistent with the measured cumulated NO_x emissions. The occurring NO_x slip at 100 s is not depicted by the NO_x storage model, further improvement of the characteristic diagrams is therefore necessary. Furthermore, the timing of the desorption from the underfloor catalyst is a little bit late. The more severe deviation is that the modelled NO_x desorption mass flow differentiates from the measured one. Altogether the NO_x storage model corresponds well with the real system behaviour, despite some minor deviations.

In order to get a comprehensive overview of the performed validation test cycles under different boundary conditions, an evaluation matrix has been established (Table 3). Overall the NO_x storage model increases the accuracy of the modelled NO_x flow during cold start for both catalyst systems. For all different driving cycles and preconditionings, an improvement in model quality has been achieved.

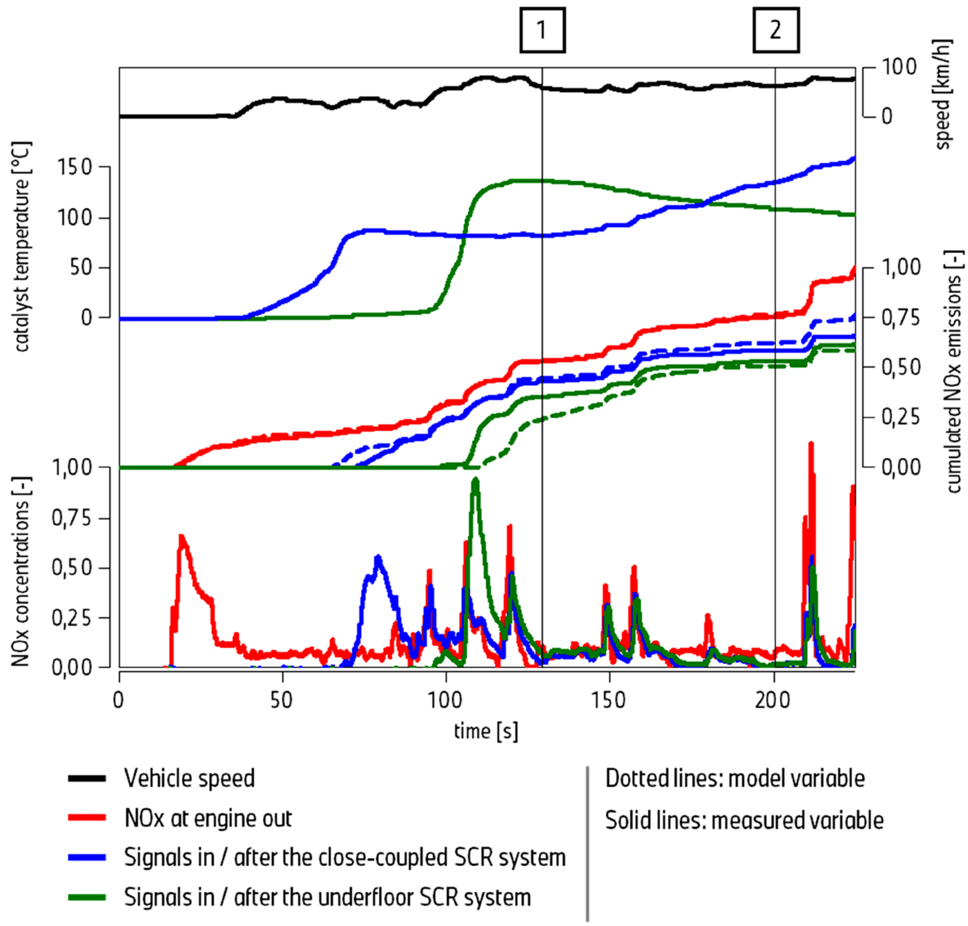

Fig. 11 RDE measurement with high dynamic preconditioning (normalized NO_x values)

● good match.
◙ slight deviation.
○ potential for improvement.

In general, there is a certain fluctuation margin which causes a potential difference between the modelled and the measured signals. Possible influence parameters are the limited measurement accuracy, variations in the engine components and the exhaust aftertreatment systems.

3 Summary and Conclusion

The aim of this paper was to model the NO_x storage behaviour during vehicle cold start for the close-coupled SCR system and the underfloor SCR system. Besides, the validation process of the model performance with the different influence parameters was outlined. These investigations pointed out that the newly implemented model of the NO_x storage behaviour significantly increased the quality of the modelled NO_x mass flow during vehicle cold start conditions.

The implemented model includes the findings of previous research work, to generate a best possible NO_x emissions modelling over the SCR catalyst systems during cold start situations. These findings include the exhaust-gas mass flow, NH_3 mass stored in the catalyst, the NO_x mass flow, the adsorbed amount of water on the catalyst, as well as the catalyst temperature as an input variable. The developed model increases the model accuracy of the SCR model in the ECU by calculating the NO_x concentrations and mass flows, as well as the corrected NH_3 mass on the catalyst in consideration of the NO_x storage behaviour. The model includes the adsorption of NO_x on the catalyst as well as the temperature driven desorption caused by water adsorption on the catalyst. The potential NO_x reduction is also taken into account by the newly developed model. The newly developed empirical model takes different boundary conditions such as influence factors from different driving styles, driving routes, ambient conditions and so on into account. This results in a prediction of the potential NO_x storage and NO_x reduction behaviour. Furthermore, relevant preconditioning cycles have been defined to evaluate the quality and limits of the NO_x storage model on a roller test bench. These different preconditioning cycles allow to evaluate the influence of different amounts of water adsorbed on the exhaust aftertreatment system. However, the model is able to generate an improvement in the signal quality for all tests that were

Table 3 Evaluation matrix of the performed validation test cycles

	Preconditioning	High dynamic cycle	Low dynamic cycle	High dynamic cycle	Low dynamic cycle	Mixed RDE driving (> 30 min)
	Driving cycle	Low dynamic city cycle	Low dynamic city cycle	High dynamic city cycle	High dynamic city cycle	Dynamic mixed RDE cycle
Close-coupled SCR system	Begin of the desorption	○	○	●	○	○
	Desorption mass flow	◙	●	●	●	●
	Converted NO_x at Cursor 1	○	◙	●	◙	●
Underfloor SCR system	Begin of the desorption	●	○	●	○	○
	Desorption mass flow	●	○	◙	●	○
	Converted NO_x at Cursor 2	●	●	●	◙	●

carried out. The resulting model has been successfully tested via RDE measurements and roller test bench measurements.

Funding Open access funding provided by Graz University of Technology.

Declarations

Conflict of interest On behalf of all authors, the corresponding author states that there is no conflict of interest.

References

1. Lao, C.T., Akroyd, J., Eaves, N., et al.: Investigation of the impact of the configuration of exhaust after-treatment system for diesel engines. Appl. Energy **267**, 114844 (2020). https://doi.org/10.1016/j.apenergy.2020.114844
2. Schmeisser, V., Weibel, M., Sebastian Hernando, L., et al.: Cold Start Effect Phenomena over Zeolite SCR Catalysts for Exhaust Gas Aftertreatment. SAE Int. J. Commer Veh **6**, 190–199 (2013). https://doi.org/10.4271/2013-01-1064
3. Reşitoğlu, İA., Altinişik, K., Keskin, A.: The pollutant emissions from diesel-engine vehicles and exhaust aftertreatment systems. Clean Techn. Environ. Policy **17**, 15–27 (2015). https://doi.org/10.1007/s10098-014-0793-9
4. Russell, A., Epling, W.S.: Diesel oxidation catalysts. Catal. Rev. **53**, 337–423 (2011). https://doi.org/10.1080/01614940.2011.596429
5. Gelbert, G., Friedrichs, O., Heß, D., et al.: NH3 -Füllstandsregelung für SCR-Katalysatoren auf Basis echtzeitfähiger physikalischer Modelle. MTZ **78**, 60–66 (2017). https://doi.org/10.1007/s35146-016-0169-2
6. Pant, A., Schmieg, S.J.: Kinetic Model of NOx SCR Using Urea on Commercial Cu−Zeolite Catalyst. Ind. Eng. Chem. Res. **50**, 5490–5498 (2011). https://doi.org/10.1021/ie200060s
7. Mora, J., Willems, F., Seykens, X., et al.: An OBD strategy to estimate SCR ageing and detect urea injection faults. IFAC-PapersOnLine **51**, 369–376 (2018). https://doi.org/10.1016/j.ifacol.2018.10.076
8. Bensaid, S., Balakotaiah, V., Luss, D.: Simulation of NO x and soot abatement with Cu-Cha and Fe-ZSM5 catalysts. AIChE J **63**, 238–248 (2017). https://doi.org/10.1002/aic.15551
9. Picerno, M., Lee, S.-Y., Pasternak, M., et al.: Real-time emission prediction with detailed chemistry under transient conditions for hardware-in-the-loop simulations. Energies **15**, 261 (2022). https://doi.org/10.3390/en15010261

10. Triantafyllopoulos, G., Katsaounis, D., Karamitros, D., et al.: Experimental assessment of the potential to decrease diesel NOx emissions beyond minimum requirements for Euro 6 Real Drive Emissions (RDE) compliance. Sci. Total Environ. **618**, 1400–1407 (2018). https://doi.org/10.1016/j.scitotenv.2017.09.274
11. Mihai, O., Tamm, S., Stenfeldt, M., et al.: Evaluation of an integrated selective catalytic reduction-coated particulate filter. Ind. Eng. Chem. Res. **54**, 11779–11791 (2015). https://doi.org/10.1021/acs.iecr.5b02392
12. Johansen K, Bentzer H, Kustov A et al. (2014) Integration of Vanadium and Zeolite Type SCR Functionality into DPF in Exhaust Aftertreatment Systems - Advantages and Challenges. In: SAE Technical Paper Series. SAE International400 Commonwealth Drive, Warrendale, PA, United States
13. Bayer T, Samuelsen D, Bareiss S et al. (2018) Double injection SCR – Bosch's development for future emission regulations. In: Bargende M, Reuss H-C, Wiedemann J (eds) 18. Internationales Stuttgarter Symposium. Springer Fachmedien Wiesbaden, Wiesbaden, pp. 579–593
14. Steinparzer F, Hiemesch D, Kranawetter E et al. (2020) Die Technik der neuen BMW 6-Zylinder-Dieselmotoren der zweiten Baukastengeneration /The Technical Concept of the New BMW 6-Cylinder 2nd Generation Modular Diesel Engines. In: Geringer B, Lenz H-P (eds) 41. Internationales Wiener Motorensymposium 22.-24. April 2020. VDI Verlag, II-34-II-53
15. Czerwinski, J., Zimmerli, Y., Mayer, A., et al.: Emission reduction with diesel particle filter with SCR coating (SDPF). Emiss. Control Sci. Technol. **1**, 152–166 (2015). https://doi.org/10.1007/s40825-015-0018-7
16. Roppertz, A., Füger, S., Kureti, S.: Investigation of urea-SCR at low temperatures. Top. Catal. **60**, 199–203 (2017). https://doi.org/10.1007/s11244-016-0597-8
17. Brandenberger, S., Kröcher, O., Tissler, A., et al.: The state of the art in selective catalytic reduction of NO x by ammonia using metal-exchanged zeolite catalysts. Catal. Rev. **50**, 492–531 (2008). https://doi.org/10.1080/01614940802480122
18. Yim, S.D., Kim, S.J., Baik, J.H., et al.: Decomposition of Urea into NH 3 for the SCR Process. Ind. Eng. Chem. Res. **43**, 4856–4863 (2004). https://doi.org/10.1021/ie034052j
19. Colombo, M., Nova, I., Tronconi, E., et al.: NO/NO2/N2O–NH3 SCR reactions over a commercial Fe-zeolite catalyst for diesel exhaust aftertreatment: intrinsic kinetics and monolith converter modelling. Appl. Catal. B **111–112**, 106–118 (2012). https://doi.org/10.1016/j.apcatb.2011.09.023
20. Grossale, A., Nova, I., Tronconi, E.: Study of a Fe–zeolite-based system as NH3-SCR catalyst for diesel exhaust aftertreatment. Catal. Today **136**, 18–27 (2008). https://doi.org/10.1016/j.cattod.2007.10.117
21. Selleri, T., Melas, A.D., Joshi, A., et al.: An overview of lean exhaust deNOx aftertreatment technologies and NOx emission regulations in the European Union. Catalysts **11**, 404 (2021). https://doi.org/10.3390/catal11030404
22. Lundström, A., Snelling, T., Morsing, P., et al.: Urea decomposition and HNCO hydrolysis studied over titanium dioxide, Fe-Beta and γ-Alumina. Appl. Catal. B **106**, 273–279 (2011). https://doi.org/10.1016/j.apcatb.2011.05.010
23. Birkhold, F., Meingast, U., Wassermann, P., et al.: Modeling and simulation of the injection of urea-water-solution for automotive SCR DeNOx-systems. Appl. Catal. B **70**, 119–127 (2007). https://doi.org/10.1016/j.apcatb.2005.12.035
24. Chen, L., Janssens, T.V.W., Skoglundh, M., et al.: Interpretation of NH3-TPD profiles from Cu-CHA using first-principles calculations. Top. Catal. **62**, 93–99 (2019). https://doi.org/10.1007/s11244-018-1095-y
25. Gao, F., Walter, E.D., Karp, E.M., et al.: Structure–activity relationships in NH3-SCR over Cu-SSZ-13 as probed by reaction kinetics and EPR studies. J. Catal. **300**, 20–29 (2013). https://doi.org/10.1016/j.jcat.2012.12.020
26. Daya, R., Joshi, S.Y., Luo, J., et al.: On kinetic modeling of change in active sites upon hydrothermal aging of Cu-SSZ-13. Appl. Catal. B **263**, 118368 (2020). https://doi.org/10.1016/j.apcatb.2019.118368
27. Gao, Z., Pihl, J., LaClair, T., et al.: Global kinetic modeling of NH3-SCR with two sites of NH3 storage on Cu-SSZ-13. Chem. Eng. J. **406**, 127120 (2021). https://doi.org/10.1016/j.cej.2020.127120
28. Tsukamoto Y, Fukuma T, Kusaka J (2019) Analysis and Modeling of NOx Reduction Based on the Reactivity of Cu Active Sites and Brønsted Acid Sites in a Cu-Chabazite SCR Catalyst. In: SAE Technical Paper Series. SAE International400 Commonwealth Drive, Warrendale, PA, United States
29. Tsinoglou, D., Koltsakis, G.: Modelling of the selective catalytic NO x reduction in diesel exhaust including ammonia storage. Proc Inst Mech Eng D **221**, 117–133 (2007). https://doi.org/10.1243/09544070JAUTO368
30. Forzatti, P., Nova, I., Tronconi, E.: New "enhanced NH 3 -SCR" reaction for NOx emission control. Ind. Eng. Chem. Res. **49**, 10386–10391 (2010). https://doi.org/10.1021/ie100600v
31. Negri, C., Selleri, T., Borfecchia, E., et al.: Structure and reactivity of oxygen-bridged diamino dicopper(II) complexes in Cu-Ion-exchanged chabazite catalyst for NH3-mediated selective catalytic reduction. J. Am. Chem. Soc. **142**, 15884–15896 (2020). https://doi.org/10.1021/jacs.0c06270
32. Iwasaki, M., Shinjoh, H.: A comparative study of "standard", "fast" and "NO2" SCR reactions over Fe/zeolite catalyst. Appl. Catal. A **390**, 71–77 (2010). https://doi.org/10.1016/j.apcata.2010.09.034
33. Ahire, V., Shewale, M., Razban, A.: A Review of the State-of-the-Art Emission Control Strategies in Modern Diesel Engines. Arch Computat Methods Eng **28**, 4897–4915 (2021). https://doi.org/10.1007/s11831-021-09558-x
34. Seykens X, Kupper F, Mentink P et al. (2018) Towards Ultra-Low NOx Emissions within GHG Phase 2 Constraints: Main Challenges and Technology Directions. In: SAE Technical Paper Series. SAE International400 Commonwealth Drive, Warrendale, PA, United States
35. Ball D, Meng X, Weiwei G (2020) Vehicle Emission Solutions for China 6b and Euro 7. In: SAE Technical Paper Series. SAE International400 Commonwealth Drive, Warrendale, PA, United States
36. Rahman, S.M.A., Rizwanul Fattah, I.M., Ong, H.C., et al.: State-of-the-Art of Strategies to Reduce Exhaust Emissions from Diesel Engine Vehicles. Energies **14**, 1766 (2021). https://doi.org/10.3390/en14061766
37. Deppenkemper K, Ehrly lng M, Schoenen M et al. (2019) Super Ultra-Low NO X Emissions under Extended RDE Conditions - Evaluation of Light-Off Strategies of Advanced Diesel Exhaust Aftertreatment Systems. In: SAE Technical Paper Series. SAE International400 Commonwealth Drive, Warrendale, PA, United States
38. Zare, A., Bodisco, T.A., Jafari, M., et al.: Cold-start NOx emissions: Diesel and waste lubricating oil as a fuel additive. Fuel **286**, 119430 (2021). https://doi.org/10.1016/j.fuel.2020.119430
39. Zare, A., Stevanovic, S., Jafari, M., et al.: Analysis of cold-start NO2 and NOx emissions, and the NO2/NOx ratio in a diesel engine powered with different diesel-biodiesel blends. Environ Pollut **290**, 118052 (2021). https://doi.org/10.1016/j.envpol.2021.118052
40. Nasello, N.D., Gramigni, F., Nova, I., et al.: AdSCR Systems (Adsorption + Selective Catalytic Reduction): Analysis of the Influence of H2O and CO2 on Low Temperature NOx Emission

Reduction Performances. Emiss Control Sci Technol **7**, 223–231 (2021). https://doi.org/10.1007/s40825-021-00204-3
41. Selleri, T., Gramigni, F., Nova, I., et al.: A PGM-free NO x adsorber + selective catalytic reduction catalyst system (AdSCR) for trapping and reducing NO x in lean exhaust streams at low temperature. Catal Sci Technol **8**, 2467–2476 (2018). https://doi.org/10.1039/c8cy00343b
42. Deinhofer, L., Maurer, M., Barnstedt, G., et al.: Analysis of the NOx storage behaviour during cold start of modern SCR flow-through substrates and SCR on-filter substrates. Automot Engine Technol (2021). https://doi.org/10.1007/s41104-021-00099-w
43. Ciardelli, C., Nova, I., Tronconi, E., et al.: Reactivity of NO/NO2–NH3 SCR system for diesel exhaust aftertreatment: Identification of the reaction network as a function of temperature and NO2 feed content. Appl. Catal. B **70**, 80–90 (2007). https://doi.org/10.1016/j.apcatb.2005.10.041
44. Colombo, M., Nova, I., Tronconi, E., et al.: Mathematical modelling of cold start effects over zeolite SCR catalysts for exhaust gas aftertreatment. Catal. Today **231**, 99–104 (2014). https://doi.org/10.1016/j.cattod.2014.01.044
45. Gramigni, F., Selleri, T., Nova, I., et al.: Analysis of AdSCR systems for NOx removal during the cold-start period of diesel engines. Top Catal. (2019). https://doi.org/10.1007/s11244-019-01138-5